# Inter-ring Torsional Modulation in Molecular Lasers. Ultraviolet Lasing via Amplified Spontaneous Emission Spectroscopy of Phenylimidazoles†

**Javier Catalán* and J. L. G. de Paz**

*Departamento de Química Física Aplicada, Universidad Autónoma de Madrid, Cantoblanco 28049, Madrid-España, Spain*

**Juan Carlos del Valle‡ and Michael Kasha*,§**

*Institute of Molecular Biophysics and Department of Chemistry, Florida State University, Tallahassee, Florida 32306-3015*

*Received: February 13, 1997; In Final Form: April 14, 1997*⊗

The intramolecularly torsion-capable molecules 2-phenylimidazole (I), 2-phenylbenzimidazole (II), 1-methyl-2-phenylimidazole (III), and 1-methyl-2-phenylbenzimidazole (IV) are shown to yield efficient UV lasing action. The *amplified spontaneous emission* (ASE) laser spikes wavelengths (and gain coefficients) are for I, 321 nm ($\alpha = 7$ cm$^{-1}$); for II, 341 nm ($\alpha = 10.5$ cm$^{-1}$); for III, 324 nm ($\alpha = 8$ cm$^{-1}$); and for IV, 345.5 nm ($\alpha = 9$ cm$^{-1}$) (ASE cell optical length of 0.8 cm). The laser spikes represent for each molecule the normal simple case of wavelength coincidence with the fluorescence maximum. Theoretical calculations are presented to correlate electronic structural changes with observed spectra and for theoretical torsional potential functions. In cases I and II, the torsional mode is active only in the excited-state $S_1$, and serves merely to modulate by a large shift ($\sim$3000 cm$^{-1}$) the ASE laser spike position, driven by stretching mode vibronic excitation. In the cases of III and IV, the torsional mode is interpreted to be the driving mode, with an ASE laser spike $\Delta\nu$ of 5000 cm$^{-1}$ or more (measured as the Franck−Condon shift of $\lambda_{max}$ from absorption to fluorescence, and the ASE laser spike position), deduced from the theoretically calculated torsional potentials offering a four-level population inversion system.

## Introduction

The 2-phenylimidazole (I), 2-phenylbenzimidazole (II), 1-methyl-2-phenylimidazole (III), and 1-methyl-2-phenylbenzimidazole (IV) molecules exhibit a strong first absorption band in the middle UV, resulting in relatively strong corresponding fluorescence bands. These properties suggested them as candidates for ASE laser spike spectroscopic research, which are shown to reveal efficient lasing at 321, 341, 324, and 345.5 nm for molecules I−IV, respectively.

This study extends our previous work on phenyloxazoles,[1,2] which proved also to be efficient in ASE laser spike generation[2] in the middle UV. In the present case of phenylimidazoles the presence of a torsional mode with its characteristic potential function introduced a possible novel feature of torsional modulation of the ASE lasing action. In both of these groups the typical four-level, two-state laser scheme is involved,[2] with the $S_0 \rightarrow S_1$ electronic transition evidencing $\pi \rightarrow \pi^*$ electronic excitation.

The four-level scheme[3] has provided spectroscopic mechanisms for the lasing action of such disparate chemical systems as the *bimolecular* processes involved in (a) the atomic-pair gaseous excimer laser[4] and (b) the molecular-pair solution excimer[5] laser as well as the *unimolecular* (intramolecular) transformation processes in such cases as (c) the excited state intramolecular proton-transfer[6] (ESIPT) laser and (d) the twisted-intramolecular-charge-transfer[7−9] (TICT) laser. Each of these processes offer substantial molecular coordinate displacement mechanisms, making available the four-level scheme. It is rational to characterize the four processes cited as involving chemical reactions in the sense that the effective species (atomic-pair excimer, molecular-pair excimer, proton-transfer (PT) tautomer, and charge-transfer twisted TICT species, respectively) are electronically distinct from the originating species.

Yet another type (e) is represented in the dye-molecule laser, in which a four-level system is achieved merely by nonequilibrium vibronic excitation conditioned by the Franck−Condon vibronic overlaps,[2,10] arising from potential curve displacement accompanying the molecular distortion upon electronic excitation. All of these cases have been analyzed previously.

A second variant of the intramolecular structural distortion as the basis for lasing action is (f) that involving an internal inter-ring torsional mode, yielding the coordinate displacement requisite for a four-level system. This mechanism has been proposed for lasing in the ultraviolet region exemplified by the case of some 2-phenylazoles.[11]

The intramolecular torsional mode in suitable molecules is one of the $3N - 6$ normal modes of a nonlinear polyatomic. The complication introduced by the presence of a torsional mode is the possibility of an energy lowering upon electronic excitation to the normal vibrational potential minimum. Figure 1 illustrates schematically a (harmonic) vibrational normal-mode potential $V(Q)$ in which excitation-induced distortion leads to a coordinate displacement along axis Q, coupled to a torsional mode potential $V(\theta)$. In a typical vibrational normal mode, stretching or bending leads to an *increase* in potential energy. In contrast, activation of an excited-state torsional mode (Figure

* Authors to whom correspondence should be addressed.

† This paper is dedicated to Professor Lionel Goodman of Rutgers University on the occasion of his 70th birthday, in celebration of his contributions on accurate vibrational potential functions and the theory of torsional potentials for molecules.

‡ Spanish Fulbright Scholar, on leave from Universidad Autonoma de Madrid, Departamento de Quimica Fisica Aplicada.

§ Work sponsored under contract No. DE-FG05-87ER60517 of the Office of Health and Environmental Research, U.S. Department of Energy, Washington, D.C.

⊗ Abstract published in *Advance ACS Abstracts,* July 1, 1997.

S1089-5639(97)00551-3 CCC: $14.00 

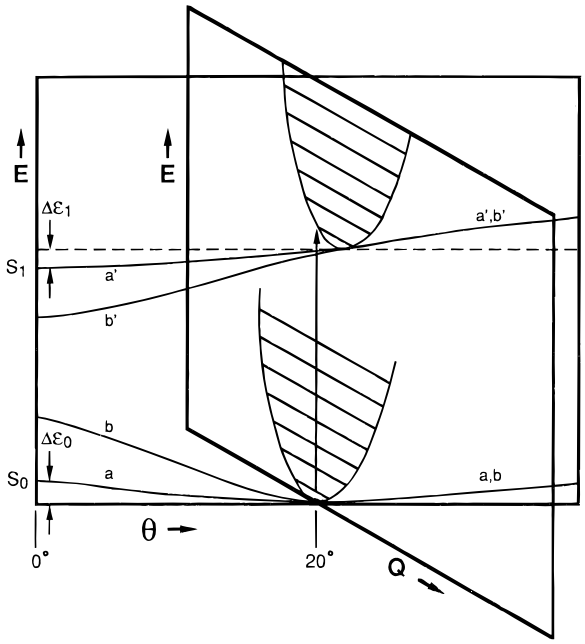


**Figure 1.** Potential energy curves diagram which represents the interplay of an average stretching/bending normal mode $V(Q)$ and a torsional normal mode $V(\theta)$.

**SCHEME 1**

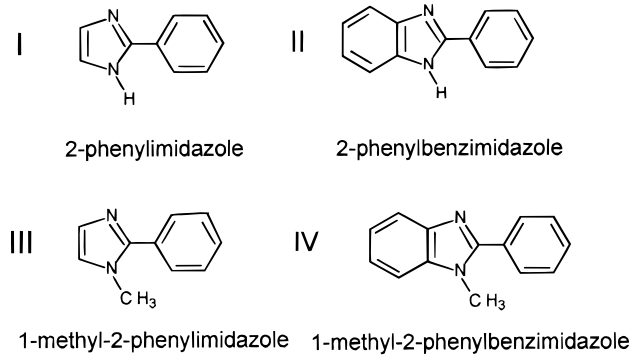


1) can lead to a *lowering* of the excited state energy. A torsional mode ground-state potential minimum upon vertical excitation commonly results in relaxation to a new torsional minimum for the lowest excited electronic state, representing a displacement along the torsional axis $\theta$. Assuming that the excitation proceeds from the equilibrium potential minimum for the $V(Q)$'s and the $V(\theta)$, the initial excitation energy $\Delta E_A(S_0 \rightarrow S_1)$ in absorption becomes in fluorescence $\Delta E_F(S_1 \rightarrow S_0) = \Delta E_A(S_0 \rightarrow S_1) - [\Delta\epsilon_0 + \Delta\epsilon_1]$.

In this paper we shall investigate for the four phenylimidazoles of Scheme 1 which of the following relations of torsional energy distortion vs stretching/bending normal-mode distortion is the operative mechanism governing the lasing action.

(A) If the energy loss term $[\Delta\epsilon_0 + \Delta\epsilon_1]$ is small compared with the displacement of the Franck−Condon maxima from the band origin, the torsional potential (curves a and a′) energy change would appear only as a modulation effect enhancing the Stokes' shift of the fluorescence band and on the possible ASE laser spike frequency. In such a case, the possibility of a four-level system is governed by the stretching normal modes,[2] with the population inversion scheme characteristic of the dye-molecule laser case (e).

(B) The case can also exist in which an excited-state torsional potential has a deep minimum, but the ground-state torsional potential is very shallow. In such a case a large Stokes shift would be observable as a modulation of the fluorescence, but the torsional potential would not be effective as the laser driving mechanism, if an ASE spike is observable.

(C) If the torsional potential minima are deep (curves b and b′), then in the four-level system the excitation dynamics can be governed by the torsional mode. In other words, the lasing conditions are present for a torsional mode if these criteria are met: (a) a large angular distortion upon excitation, (b) a deep excited-state and ground-state torsional minima, and (c) Franck−Condon selection of nonequilibrium ground-state torsional modes upon fluorescence. When these conditions are matched, a population inversion can result with subsequent lasing emission. We could then characterize the laser as a torsionally induced laser.

## Experimental Section

**Steady-State Spectroscopy.** The spectroscopic observations were made for the various phenylimidazoles in solution at 298 K in the concentrations and solvents given in the text and the figure legends. The absorption spectra were recorded by a Shimadzu UV-2100 spectrophotometer. Fluorescence spectra (corrected) were obtained from an AB2 Aminco-Bowman Series 2 luminescence spectrometer. The first fluorescence peak appears to be very sensitive to slit width and the sample concentration because of strong self-absorption. All the fluorescence spectra were measured by using 4 and 0.5 nm slits in the excitation and in the emission monochromators, respectively.

**ASE Spectroscopy.** The ASE laser spike measurements (cf. ref 2) were made by primary excitation with a Nd:YAG laser (Spectra-Physics Model DCR-3G), using the fourth harmonic (266 nm) for 2-phenylimidazole, 2-phenylbenzimidazole, and 1-methyl-2-phenylbenzimidazole. The output of the Nd:YAG laser was focused to a narrow line in the dye cell in a transverse geometry. A Molectron DL 251 laser dye cell of 0.8 cm optical length was used, with oblique windows designed to prevent optical feedback. The dye solution was stirred to prevent secondary processes (local heating, triplet population, etc.) from interfering with the experiments. The amplified spontaneous emission (ASE) was dispersed by a 300 lines/mm and 0.32 m polychromator (Instruments SA Model HR320), detected by an optical multichannel analyzer (OMA) system consisting of an intensified silicon photodiode array (EG&G/PAR, Model 1421), and analyzed by a system processor (EG & G/PAR, model 1461/1463). To reduce the noise, the detector was operated in a gated-mode synchronously with the Nd:YAG laser. The ASE was detected through a pinhole 0.05 cm in diameter placed at a distance of ca. 50 cm from the sample cell.

It should be pointed out that the ASE laser spikes and their respective gain coefficients were measured in a mirrorless cavity,[12] without feedback from the windows of the cuvette. To measure the gain coefficient values, an optically calibrated half-cell shutter was placed between the primary laser excitation and the cell to block half the intensity of the excitation beam. The intensities of the primary laser excitation at the respective full-cell length and half-cell length of the shutter were optically calibrated with a volume absorbing disk calorimeter (Scientech, Inc., Model 36-0001).

In the laser experiments, the solutions were degassed by bubbling Ar gas through the small oblique-windowed ASE laser cell for 30 min prior to excitation. Photoinstability was negligible during the experimental time. Photostability of the compounds studied was demonstrated by monitoring the absorption spectra before and after the laser experiments, using a cuvette of 0.01 cm optical length.

The 2-phenylimidazole (I), 2-phenylbenzimidazole (II), and 1-methyl-2-phenylbenzimidazole (IV) (Scheme 1) were purchased from Aldrich Chemical Co. and used as supplied. The

1-methyl-2-phenylimidazole (III) molecule was a gift of Dr. R. M. Claramunt. All the solvents used were spectrophotometric grade.

**Theoretical Calculations.** Both ground-state ($S_0$) and first singlet excited-state ($S_1$) geometries were optimized using a 6-31G** basis set with the Gaussian 94[13a] program. The $S_0$ geometry was calculated at the SCF level, and the $S_1$ geometry was obtained by means of a CIS method[14] due to the size of our systems. The geometry of the $S_1$ was fully optimized using the Berny algorithm.[15] The program Spartan 4.1[13b] was used for visualizing the vibrations. The harmonic vibrational frequencies ($cm^{-1}$) were multiplied by a scaling factor of 0.8953.[16] The six molecular geometries calculated for the molecules I, II, and IV are assigned to minima, because each of them possesses $3N - 6$ vibrational modes with positive frequencies.[17] Calculations for molecule III were unavailable (cf. Table 2), as the newly synthesized sample was available after this paper was completed.

## Equilibrium Spectroscopy of the Phenylimidazoles

Among organic species which can act as laser materials, the 2-phenylimidazole (I), 2-phenylbenzimidazole (II), 1-methyl-2-phenylimidazole (III), and 1-methyl-2-phenylbenzimidazole (IV) molecules are examples that can undergo an intramolecular inter-ring torsional distortion in their chemical structure upon excitation (Figure 1). Such species consequently may exhibit novel spectral properties in their lasing action. In the cases at hand, electronic excitation upon UV light absorption of the equilibrium nonplanar conformation in the ground electronic state $S_0$ (as depicted in Figure 1) at the appropriate wavelength leads to the lowest torsionally nonequilibrated singlet excited-state $S_1$, whereupon a barrierless inter-ring torsional motion yields a planar conformation which subsequently may emit fluorescence.

We shall first present the equilibrium absorption spectroscopic results, for the four molecules under study, including examination of the lasing capacity for the four species. This will be followed by presentation of the results of theoretical molecular calculations which can serve as the bases for interpretation of the potential energy diagrams and the expected excited-state behavior as lasers. We shall then interpret the molecular lasing behavior on the basis of the theoretically calculated torsional potential energy function. This step is critical and adds an essential component to the interpretation of the possible role of a molecular torsional potential in facilitating an excited-state population inversion as a torsionally driven lasing action.

**UV Absorption and Fluorescence Spectra.** The first UV absorption region and corresponding (corrected) fluorescence emission spectra of 2-phenylimidazole (I) in *n*-pentane and in dioxane solution at 298 K are given in Figure 2. Analogous data for 2-phenylbenzimidazole (II) are given in Figure 3, and for 1-methyl-2-phenylbenzimidazole (IV) in Figure 4. The unusual character of the Franck−Condon absorption spectral envelope and the appearance of the vibronic structure for the room temperature *n*-pentane solution of I suggests strongly that for this case the absorption band consists of two superposed electronic transitions (cf. Table 2), unlike molecules II−IV.

The UV absorptions are intense, guaranteeing short fluorescence lifetimes by the Einstein $A_{21}/B_{12}$ coefficient relation, as indicated by the molar absorption coefficients values ($\epsilon$) of log $\epsilon = 4.25$ at 275 nm for I, log $\epsilon = 4.37$ at 304 nm for II, and log $\epsilon = 4.25$ at 293 nm for IV. The $\epsilon$ coefficients values were calculated for the compounds studied in dioxane solutions. There is a striking contrast in the relation of the absorption and fluorescence spectra of III and IV compared to phenylimidazoles I and II (cf. Table 2). A fundamental difference in torsional

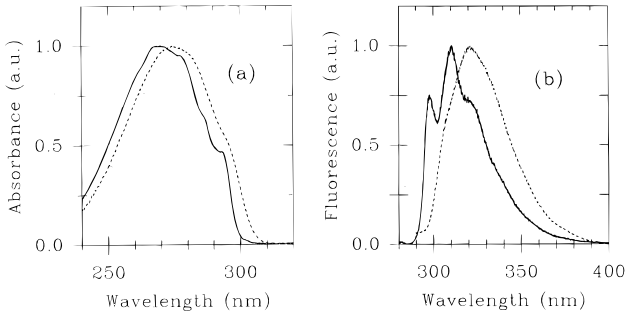


**Figure 2.** (a) Absorption spectra of 2-phenylimidazole in *n*-pentane and dioxane (- -). (b) Emission spectra of 2-phenylimidazole in *n*-pentane and dioxane (- -) solutions upon excitation at 260 nm, $1.7 \times 10^{-6}$ M.

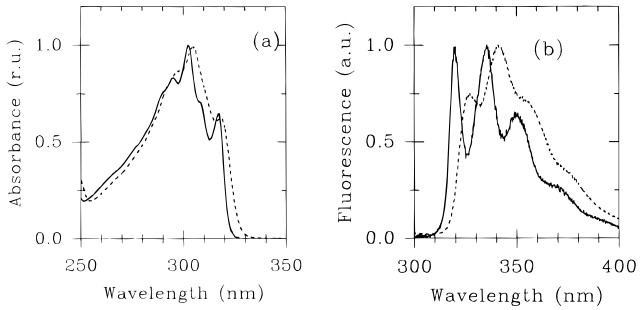


**Figure 3.** (a) Absorption spectra of 2-phenylbenzimidazole in *n*-pentane and dioxane (- -). (b) Emission spectra of 2-phenylbenzimidazole in *n*-pentane and in dioxane (- -) solutions upon excitation at 270 nm, $1.3 \times 10^{-6}$ M.

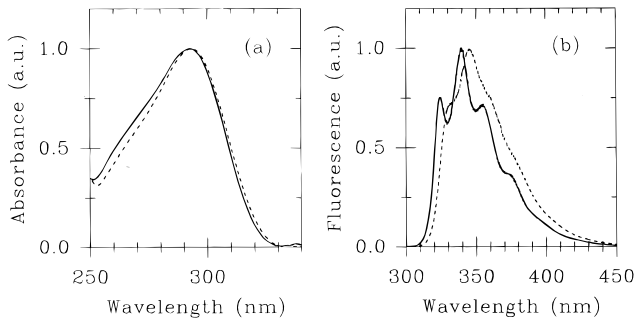


**Figure 4.** (a) Absorption spectra of 1-methyl-2-phenylbenzimidazole in *n*-pentane and dioxane (- -). (b) Emission spectra of 1-methyl-2-phenylbenzimidazole in *n*-pentane and in dioxane (- -) solutions ($1.7 \times 10^{-6}$ M) upon excitation at 270 nm.

effects in these cases will be presented in the discussion−interpretation section.

The spectra reveal the usual increased spectral broadening of both the absorption and fluorescence bands in comparing dioxane with *n*-pentane as the solvent. There is also the small dispersion red-shift in both absorption and fluorescence spectra. The striking general feature, however, is the considerable increase in vibronic structure in the fluorescence spectrum of all the molecules studied compared with their absorption contours, most evident in the hydrocarbon solutions. This last feature will prove to be a consequence of especially prominent torsional modes in the $S_1$ excited states. The band half-widths (fwhm) show contrasts (cf. Table 2), also, that for the fluorescence band being smaller than the half-width of the corresponding absorption band for the four phenylimidazoles. For instance, the fluorescence half-widths ($cm^{-1}$) are about 1950, 640, 1790, and 2300 smaller than the corresponding absorption half-widths for 2-phenylimidazole (I), 2-phenylbenzimidazole (II), 1-methyl-2-phenylimidazole (III), and 1-methyl-2-phenylbenzimidazole (IV), respectively (cf. Table 2, and Discussion). In this case again, these observations will be related to a

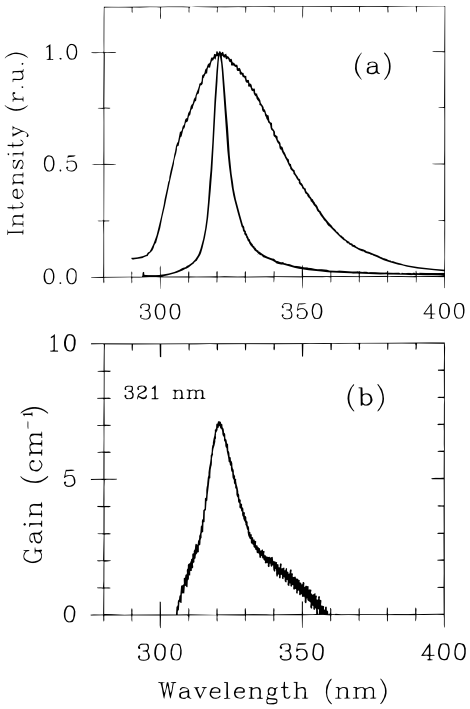


**Figure 5.** (a) Fluorescence ($1.7 \times 10^{-6}$ M) and amplified spontaneous emission (ASE) of 2-phenylimidazole ($3.2 \times 10^{-3}$ M) in dioxane at 298 K. (b) ASE gain spectrum for 2-phenylimidazole ($3.2 \times 10^{-3}$ M) in dioxane (298 K) upon excitation at 266 nm. The excitation energy was 30 mJ.

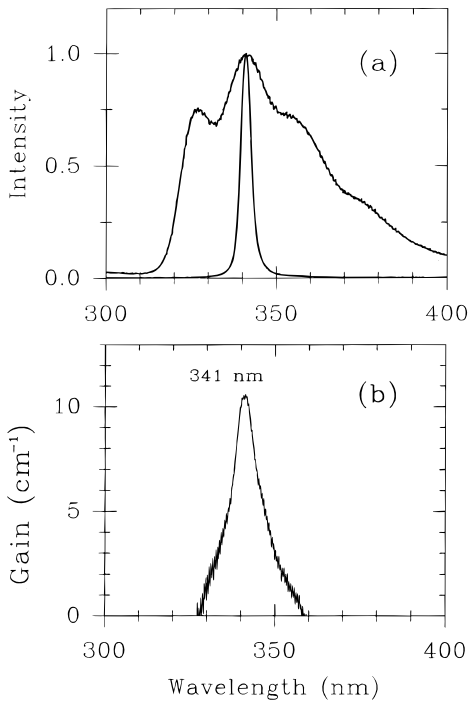


**Figure 6.** (a) Fluorescence ($1.3 \times 10^{-6}$ M) and amplified spontaneous emission (ASE) of 2-phenylbenzimidazole ($2.0 \times 10^{-3}$ M) in dioxane at 298 K. (b) ASE gain spectrum for 2-phenylbenzimidazole ($2.0 \times 10^{-3}$ M) in dioxane (298 K) upon excitation at 266 nm. The excitation energy was 30 mJ.

difference in the torsional mode excitation in the $S_1$ state vs the $S_0$ state, in our discussion−interpretation section.

**Amplified Spontaneous Emission (ASE) Spectroscopy.** The limited solubility of the 2-phenylimidazole and 2-phenylbenzimidazole molecules in inert hydrocarbon solvents such as *n*-pentane, cyclohexane, methylcyclohexane, and decalin does not allow preparation of solutions sufficiently concentrated in these to give rise to lasing action. Therefore, the ASE laser experiments were carried out for dioxane solutions, in which the four phenylimidazole molecules (I−IV) present a sufficient solubility.

The ASE laser spikes were observed and recorded for highly concentrated solutions of the phenylimidazoles in dioxane ($2.0 \times 10^{-3}$ M) and appear at 321 nm for 2-phenylimidazole (I, Figure 5a), 341 nm for 2-phenylbenzimidazole (II, Figure 6a), 324 nm for 1-methyl-2-phenylimidazole (III; cf. Table 2), and 345.5 nm for 1-methyl-2-phenylbenzimidazole (IV, Figure 7a), respectively. The ASE laser spikes show up at or very close to the maxima of the fluorescence spectra, as required by normal physical optics and the exponentiality of the laser-induced excitation wave train. The exponential character of the amplification of the light reinforces the most strongly emitting level and leads to the relative suppression of the weaker emitting components of the original fluorescence band. The result is the typical ASE laser spike narrowing compared with the original fluorescence band. The ASE laser spike cannot emerge at the position of the 0−0 transition, because that would correspond to a two-level system, for which population inversion is not achievable. The strong self-absorption of the 0−0 emission band region arising from the intense absorption does not interfere in our case with the ASE laser spike emission. The Franck−Condon maximum in these cases generally occurs at ca. 3000 cm$^{-1}$, from the fluorescence onset, safely removed from the 0,0 region.

The molecules I−IV show high gain coefficient values (ASE cell $L = 0.80$ cm), $\alpha = 7$ cm$^{-1}$ at 321 nm (Figure 5b), $\alpha = 10.5$ cm$^{-1}$ at 341 nm (Figure 6b), $\alpha = 8$ cm$^{-1}$ at 324 nm, and

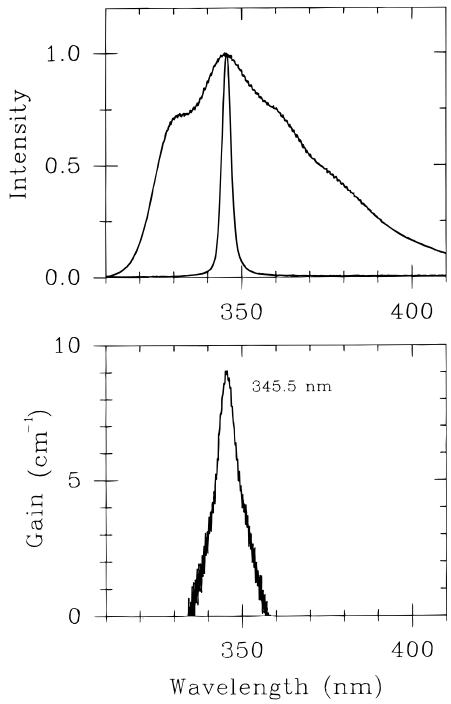


**Figure 7.** (a) Fluorescence ($1.7 \times 10^{-6}$ M) and amplified spontaneous emission (ASE) of 1-methyl-2-phenylbenzimidazole (0.01 M) in dioxane at 298 K. (b) ASE gain spectrum for 2-phenylbenzimidazole (0.01 M) in dioxane (298 K) upon excitation at 266 nm. The excitation energy was 30 mJ.

$\alpha = 9$ cm$^{-1}$ at 345.5 nm (Figure 7b), respectively, coinciding with the peak position of their ASE laser spikes. The 2-phenylimidazole molecule lases at UV wavelengths even shorter than those measured for the 2-phenylbenzoxazole compound at the same experimental conditions.[1,2]

The observation of an ASE laser spike at 321 nm for 2-phenylimidazole represents the shortest UV laser wavelength to date for dye-molecules without subsidiary tuning effects.

**SCHEME 2**

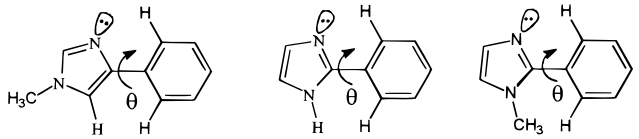


**SCHEME 3**

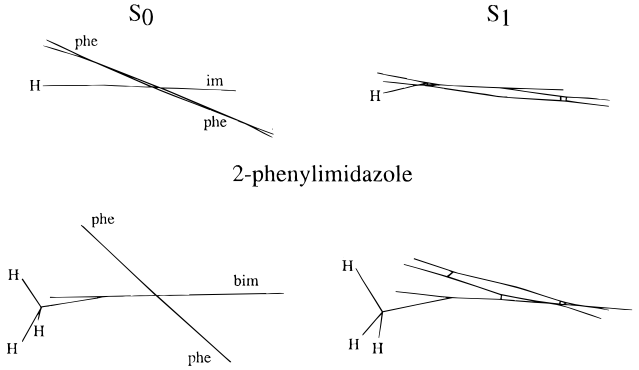


Furthermore, if the 2-phenylimidazole molecule were dispersed up to $10^{-3}$ M in concentration in a medium with low polarity-polarizability as that for *n*-pentane, it would generate a laser spike shifted about 12 nm to the blue with regard to the laser spike found in dioxane.

The compounds studied clearly exhibit good UV lasing properties in dioxane. The four phenylimidazole molecules follow a four-level, two-state mechanism, which enables them to lase from a coplanar or almost coplanar conformation in the first singlet excited state. However, in the discussion and interpretation section, we shall consider the particular effect of the torsional motion as a *modulation* effect rather than a driving effect in some of the phenylimidazole cases.

### Theoretical Calculations

The ab initio calculated geometries of the 2-phenylimidazole (I), 2-phenylbenzimidazole (II), and 1-methyl-2-phenylbenzimidazole (IV) molecules for their ground electronic state are nonplanar, with inter-ring torsional angles of 19°, 20°, and 42°, respectively. The nonplanarity of all the molecules in their $S_0$ state is caused primarily by an electrostatic and a steric repulsion between the pyrrolic hydrogen (for I and II) or the pyrrolic methyl (for IV) in the heterocyclic ring and the hydrogen atom in the ortho position of the phenyl ring. The X-ray geometries of 1-methyl-4-phenylimidazole and the 1-methyl-2-phenylimidazole (III) molecule,[18] support the above interpretation, as seen by comparing their inter-ring torsional angles ($\theta$) to 7.3° and 32.3°, respectively, to the 19° value calculated for I (Scheme 2).

In the three molecules studied (I, II, and IV), our theoretical calculations indicate that the $S_1$ ($\pi\pi^*$) equilibrium geometry changes toward a coplanar conformation. That coplanar conformation is completely reached by the 2-phenylbenzimidazole molecule with an inter-ring torsional angle of $\theta = 0.0°$, and almost reached by the 2-phenylimidazole with $\theta = 1.9°$ and the 1-methyl-2-phenylbenzimidazole with $\theta = 2.0°$ (cf. Scheme 3).

To diminish the steric interaction, the pyrrolic methyl in the 1-methyl-2-phenylbenzimidazole molecule forces the twisting of the phenyl ring with regard to the benzimidazole ring to ca. 9°. However, the torsional angle between the phenyl and the benzimidazole rings is only 2°. In addition, the pyrrolic methyl is out of the benzimidazole plane (cf. Scheme 3).

These coplanar conformations produce a shortening of the intercyclic C−C distance (cf. Scheme 4), which reinforces its double bond character, and an increase of the (theoretical) oscillator strength $f_{S_0 \rightarrow S_1}$ (at ∼20°) for absorption versus $f_{S_1 \rightarrow S_0}$ (planar) for emission (i.e., from 0.54 ($f_{S_0 \rightarrow S_1}$) to 0.74 ($f_{S_1 \rightarrow S_0}$) for I, from 0.75 ($f_{S_0 \rightarrow S_1}$) to 1.05 ($f_{S_1 \rightarrow S_0}$) for II, and from 0.59 ($f_{S_0 \rightarrow S_1}$) to 1.03 ($f_{S_1 \rightarrow S_0}$) for III), in agreement with parallel results in our previous paper.[11]

It is noteworthy that the $S_1$ geometry of 2-phenylimidazole represents a loss of planarity in the imidazole ring, because of a slightly pyramidal conformation brought about by the pyrrolic nitrogen. That pyramidal conformation diminishes the repulsion between the pyrrolic hydrogen and the hydrogen atom in the ortho position of the phenyl ring. The pyrrolic hydrogen adopts an angle of 18° with regard to the imidazole plane (Scheme 3). For the molecule IV all the above-mentioned conformational features are reinforced (cf. Scheme 3).

It is noteworthy that the fundamental vibrations assigned to an intercyclic torsion increase their frequency in the $S_1$ state. Thus, the vibration $\nu_1(S_0) = 42.1$ cm$^{-1}$ goes up to $\nu_2(S_1) = 98.9$ cm$^{-1}$ in 2-phenylimidazole, $\nu_1(S_0) = 37.4$ cm$^{-1}$ increases to $\nu_2(S_1) = 63.4$ cm$^{-1}$ in 2-phenylbenzimidazole, and $\nu_1(S_0) = 47.5$ cm$^{-1}$ is raised to $\nu_3(S_1) = 100.1$ cm$^{-1}$ for 1-methyl-2-phenylbenzimidazole. This statement denotes that those vibrational modes will be less populated in the $S_1$ state, favoring the shortening of the inter-ring C−C bond by increasing its double bond character.

Scheme 4 reveals C−C distances within the phenyl group to be very much alike in the ground state of all the compounds studied. This similarity can be ascribed to the phenyl group acting as an independent benzene ring. In contrast, the C−C distances of the phenyl group in the corresponding $S_1$ state are quite different from each other, denoting that a significant resonance effect appears between the rings upon going to a planar conformation. Scheme 4 shows important structural parameters of the compounds studied in the $S_0$ and the $S_1$ electronic states.

The rotational constants, dipole moments and polarizabilities for all of the calculated electronic states are gathered in Table 1. It is worth mentioning that polarizability increases significantly upon excitation in the three molecules (I, II, and IV). The dipole moment changes upon excitation only slightly in magnitude but its orientation changes significantly (Scheme 5). Because of these dipole changes in orientation, a solvent relaxation effect upon $S_0$ to $S_1$ excitation dependent on solvent polarity is expected for 2-phenylimidazole, 2-phenylbenzimidazole and 1-methyl-2-phenylbenzimidazole.

In summary, the primary effects upon electronic excitation are a shortening of the inter-ring C−C bond distances, an increase of the intercyclic torsional frequency, a differing oscillator strength for the $S_1 \rightarrow S_0$ versus that for the $S_0 \rightarrow S_1$ electronic transitions (for the four-level system; cf. Figure 1), and the reorientation of the dipole moment. All the latter phenomena demonstrate a reinforcement of the coplanar conformation between the phenyl group and the heterocyclic rings in the first singlet excited state.

### Discussion and Interpretation of Results

The experimental results presented in this paper show that the four phenylimidazole molecules under study can function as highly efficient UV lasers in the spectral region from 300 to 340 nm with gain coefficients in the range $\alpha = 7-10$ cm$^{-1}$

**SCHEME 4**

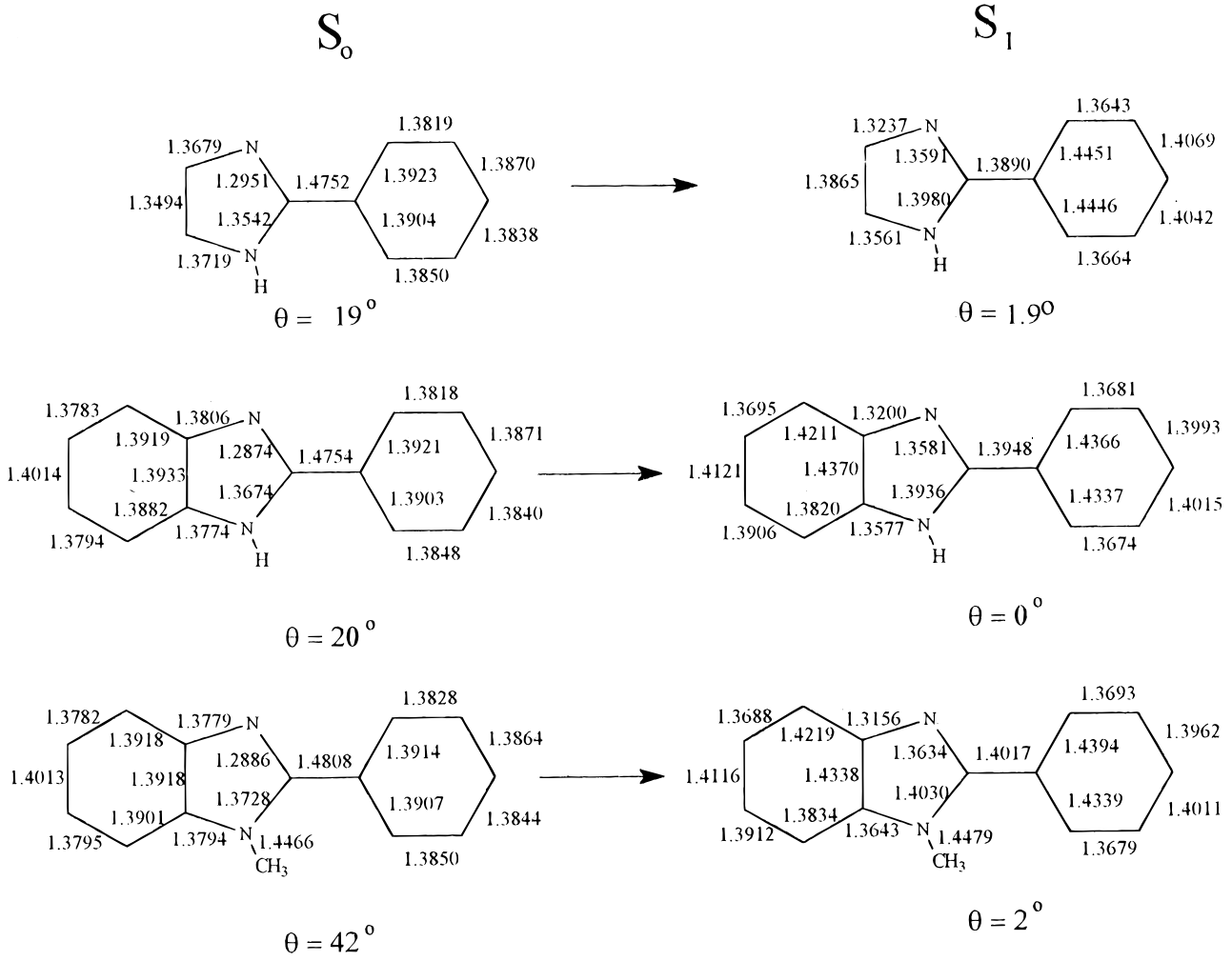


**TABLE 1: Rotational Constants (MHz), Total Dipole Moment (debye), and Its Components on the Inertial Axis and the Molecular Polarizability (F m$^2$) of the Compounds Studied for Both the Ground Electronic State ($S_0$) and the First Excited Electronic State ($S_1$)**

| compound | electronic state | rotational constant (MHz) | | | dipole moment (debye) 6-31G** | | molecular polarizability (F m$^2$) |
|---|---|---|---|---|---|---|---|
| | | *A* | *B* | *C* | $\mu$ | $\mu_a$, $\mu_b$, $\mu_c$ | |
| 2-phenylimidazole | $S_0$ | 3623.6 | 703.8 | 594.6 | 3.35 | −0.38, −3.21, +0.90 | 94.40 |
| | $S_1$ | 3461.0 | 717.6 | 594.8 | 3.58 | +1.64, −3.13, +0.57 | 124.64 |
| 2-phenylbenzimidazole | $S_0$ | 2371.5 | 308.3 | 274.8 | 3.33 | −1.46, −2.90, +0.72 | 138.27 |
| | $S_1$ | 2302.4 | 311.9 | 274.7 | 3.02 | +0.67, −2.95, +0.00 | 199.04 |
| 1-methyl-2-phenylbenzimidazole | $S_0$ | 1646.3 | 302.2 | 265.4 | 3.71 | −1.50, −3.27, +0.90 | 147.26 |
| | $S_1$ | 1571.2 | 309.7 | 261.0 | 3.27 | +0.79, −3.15, +0.39 | 207.73 |

[a] All these values have been calculated at the SCF level with a 6-31G** basis set.

**TABLE 2: Spectroscopic Summary on Imidazoles**

| | molecule | Stokes' shift (cm$^{-1}$) | $\Delta(\Delta\nu_{1/2})$ (cm$^{-1}$)[a] | ASE spike (dioxane) (nm) |
|---|---|---|---|---|
| I | 2-phenylimidazole | (4800)[b] | (1950)[b] | 321 |
| II | 2-phenylbenzimidazole | 3300 | 640 | 341 |
| III | 1-methyl-2-phenylimidazole[c] | 5600 | 1790 | 324 |
| IV | 1-methyl-2-phenylbenzimidazole | 5000 | 2300 | 345.5 |

[a] The symbol $\Delta(\Delta\nu_{1/2})$ means difference in band half-width (fwhm) for the first absorption band minus that for the fluorescence band. [b] The first absorption band for this molecule has a clear indication (cf. Figure 2) of consisting of two superimposed transitions excaggerating the magnitude of the datum. [c] Catalan, J.; del Valle, J. C.; Kasha, M.; Claramunt, R. M., manuscript in preparation.

**SCHEME 5**

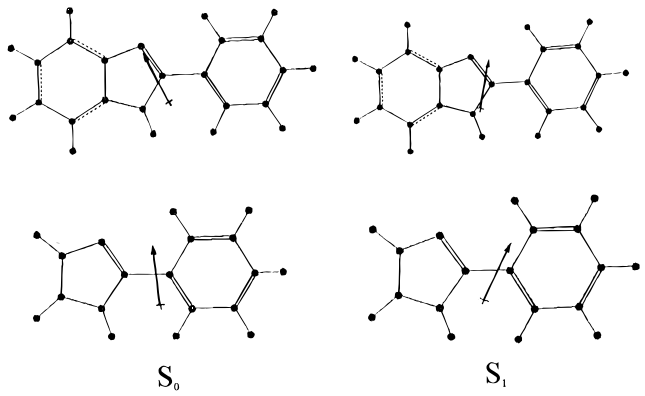


(ASE cell $L = 0.80$ cm). This section will deal with the role of the torsional potential in the ASE laser spike spectroscopy.

The torsional potential introduces Mathieu functions as torsional eigenfunctions.[19] In the Franck−Condon integrals the

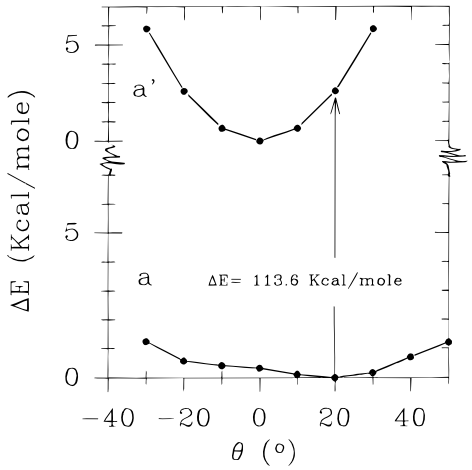


**Figure 8.** Theoretical potential energy curves for the 2-phenylbenzimidazole molecule (cf. theoretical calculations).

effect of these eigenfunction overlaps is to shift the band maximum far from the origin, as the 0,0 torsional overlap is always zero. Torsional potentials are thus the most common cause of an enhanced Stokes shift between absorption and fluorescence maxima, compared with the shift observed for nontorsionally capable molecules. The F−C band contour also is affected directly. We refer to these spectroscopic influences as the *torsional potential modulation effect.*

It is notable that the ASE laser spikes in the four imidazoles studied exhibit the simplest type of behavior relative to their originating fluorescence bands: the laser spikes are narrow, symmetrical and coincide with the fluorescence band maximum. This behavior is analogous to the case of the 2-phenylbenzoxazole[1,2] but strikingly different from that of the more complex binary-structured phenyloxazoles, which yield ASE laser spikes at weaker subsidiary fluorescence vibronic bands. The behavior is also different from that of the polyhydroxyflavones[20] which show ASE laser spikes red-shifted of up to 1000 $cm^{-1}$ relative to the normal fluorescence maxima.

**Torsional Mode Modulation Effect on Lasing.** The schematic potential curves of Figure 1 show contrasting cases of torsional potentials, both $S_0(\theta)$ and $S_1(\theta)$ potentials having shallow minima (curves a and a′), or both $S_0(\theta)$ and $S_1(\theta)$ potentials having deep minima (curves b and b′), with barriers in these latter cases far above *kT*.

The theoretically calculated potential for 2-phenylbenzimidazole is given in Figure 8. The ground-state $S_0$ has a very shallow torsional potential, with a minimum (cf. Scheme 4) at $\theta = +20°$, lying 0.33 kcal/mol (115 $cm^{-1}$) below the value at $\theta = 0°$. One could expect a second minimum at $\theta = -20°$, with an energy equivalent to the minimum at $\theta = 20°$. However, the computational procedure is carried out for the skeletal geometry relaxed only to the angle $\theta = +20°$, so the equilibrium symmetry of the potential does not appear, and the barrier maximum is not defined. There are two other minima expected at $\theta = \pi \pm 20°$ in this periodic torsional potential. As explained in the theoretical section, the origin of the low barrier for torsion in this case is in the phenyl ortho-H-atom repulsion with nitrogen-H atom of the imidazole ring, which spatially represents a weak steric and protic repulsion. The inter-ring C−C bond length (Scheme 4) in the $S_0$ states is 1.475 Å approaching the classic C−C bond length of 1.54 Å for unsaturated aliphatic molecules, corresponding to nearly pure single-bond character.

The excited states $S_1$ however exhibit coplanarity with potential minima at $\theta = 1.9°$ for 2-phenylimidazole (I) and 0° for 2-phenylbenzimidazole (II, Scheme 4). The inter-ring C−C bond lengths here are calculated to be 1.389 and 1.395 Å for molecules I and II, respectively. These are the classical aromatic C═C bond lengths. As discussed in the theoretical calculations section, the deep $S_1(\theta)$ potential minimum owes its torsional dependence to overcoming the barrier to double bond twisting. It will be noted that the entire electronic structure in the excited-state trends toward a quinonoid structure over the 2-ring skeleton. These are two such torsional minima in the $S_1$ state in the range $0-2\pi$, one at $\theta = 0°$, and the other at $\theta = 180°$.

It is clear however, that when the molecule is excited from the ground-state minimum at $\theta = 20°$ in these molecules, although thermal equilibration brings the molecule to a new minimum at 0° in the $S_1(\theta)$ potential (with the $S_1(Q)$ normal modes following), the torsional potential by itself cannot yield a lasing mechanism in the present case with torsional potentials represented by the curves in Figure 8 (curves a and b′ of Figure 1; case B of the Introduction). It is obvious that light emission from $S_1(\theta=0°,\upsilon'=0) \rightarrow S_0(\theta=0°)$ puts the molecule in Boltzmann equilibrium with the $S_0(\theta=20°,\upsilon=0)$. Thus, criterion (c) of the Introduction conditions is not met, and the torsional potentials in such a case constitute a 2-level system and which cannot yield a population inversion. The observed lasing action of the phenylimidazoles must therefore lie in a fundamental mechanism involving the Franck−Condon governed transitions of the V(Q) stretching normal modes[2] in the dye-molecule laser mechanism (e).

We now examine the torsional mode modulation effect on the laser characteristics of the molecule 2-phenylbenzimidazole. The relationship of the $S_1(\theta)$ and $S_0(\theta)$ potentials indicates as stated that the torsional mode in this case can only serve as a modulation not a driving mechanism on the lasing action.

Table 2 presents a summary of spectroscopic data on the four imidazoles. Comparing the absorption spectra and fluorescence spectra of Figures 2−4 it appears that the absorption band for 2-phenylimidazole (I) may represent two superimposed electronic transitions. Thus, the band half-width (fwhm) and the Stokes shifts for this molecule are exaggerated and are placed in parentheses. It is clear, that the presence of a torsional mode greatly broadens the apparent first absorption band, and shifts the Franck−Condon maximum away from the band 0,0 origin. This latter effect appears in an enhanced Stokes shift. However, the torsional potential calculation for these molecules clearly indicates a relatively flat torsion potential in the ground electronic state. Therefore, we conclude that although the excitation of the torsional mode in the excited state of molecules I and II modulates the ASE lasing action and imparts a very substantial Stokes shift (∼3000 $cm^{-1}$) to the laser spike (measured on the ASE spike displacement from the F−C absorption maximum), it cannot constitute the laser driving mechanism.

**Torsionally Induced ASE Laser Mechanism.** In the simple torsional-modulation laser mechanism case it was shown that although the first absorption band in such molecules has a considerably greater band half-width $\Delta\nu_{1/2}$ (fwhm), the corresponding fluorescence band is generally much narrower and usually exhibits more vibronic structure. Table 2 summarizes the comparisons for the four imidazoles. This general feature of greater absorption band half-width and general obliteration of vibronic structure comes about from the superposition of Franck−Condon overlap integration in torsionally capable molecules over both torsional eigenfunctions and stretching/bending vibrational eigenfunctions of the upper state $S_1$. However, as would be clear from Figure 1, molecules such as I and II, having very shallow $S_0$ torsional potentials (cf. Figure 8 for II), cannot develop population inversion dominated by the torsional mode. Therefore, only a dominant normal vibration mode is available to develop a four-level, two-state mechanism for lasing action. The torsional mode serves in that case to merely enhance the apparent Stokes shift of the ASE laser spike

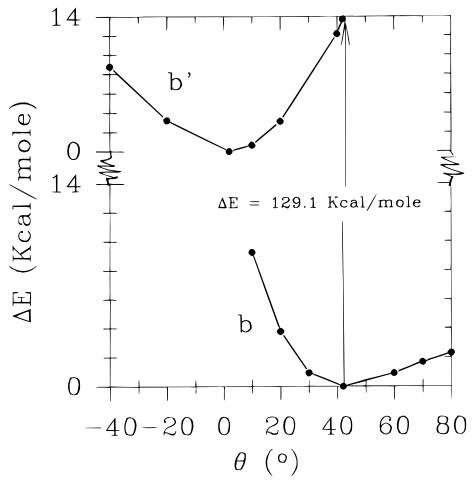


**Figure 9.** Theoretical potential energy curves for the 1-methyl-2-phenylbenzimidazole molecule (cf. theoretical calculations).

relative to the absorption $\lambda_{max}$. In contrast, molecules III and IV should have a hindered torsional mode as a consequence of the ortho-methyl substitution. This is confirmed by calculations for molecule IV (cf. Figure 9), and although analogous results are not yet available for molecule III, the parallelism in structure can be expected to lead to a similar result. Thus, as the comparison in Table 2 indicates, exceptionally large absorption band half-widths for molecules III and IV are observed, with correspondingly enhanced Stokes shifts ($\sim$5000 cm$^{-1}$) of their fluorescence bands. Thus, for molecules III and IV population inversion can be achieved via the torsional potential because the ground-state torsional potential also has a significant potential depth (cf. Figure 9). Thus, we interpret this case as satisfying the three criteria given in the introduction for a *torsionally driven lasing mechanism* (case C of the Introduction). The large coordinate change arising from the torsional mode distortion must dominate the coordinate change expected for a stretching/bending vibrational mode in a polyatomic molecule.

An interesting parallel exists in the TICT mechanism. This is defined as the twisted-intramolecular-charge-transfer phenomenon. It is clear however, in view of discussion of this paper, that TICT could be translated as *torsionally induced charge-transfer*, as the Godfrey−Murrell potential[21] leads to the diabatic interaction of an upper charge-transfer state with the lowest excited $\pi,\pi^*$ excited state.[22] Thus, the TICT laser is another example of a torsionally driven lasing mechanism.

## Conclusion

The four phenylimidazoles studied in this paper, 2-phenylimidazole (I), 2-phenylbenzimidazole (II), 1-methyl-2-phenylimidazole (III), and 1-methyl-2-phenylbenzimidazole (IV), prove to be efficient UV *amplified spontaneous emission* (ASE) laser spike generators, with 2-phenylimidazole exhibiting the shortest UV molecular laser wavelength (321 nm) observed to date for any organic molecule. The ASE laser spikes conform to the normal simple physical optics case of wavelength coincidence with the Franck−Condon fluorescence maximum, the laser spike narrowing resulting from successive exponential induced emission steps in the mirrorless laser cavity. The main purpose of the research was to investigate the role of the internal torsional potential in the ASE lasing mechanism. Theoretical calculations were carried out to estimate electronic structural changes upon excitation correlated with the observed spectra, interpreted on the basis of theoretical torsional potentials.

It was found that molecules I and II, for which the theoretically calculated potentials showed only a shallow minimum for the $S_0$ ground state and a somewhat deeper minimum for the $S_1$ excited state. These torsional potential relations resulted in only a modulation, exhibited as a large Stokes shift ($\sim$3000 cm$^{-1}$) of the vibronically driven lasing action. In contrast, molecule III and molecule IV, for which case the theoretically calculated torsional potentials exhibited deep minima in both the ground-state $S_0$ and the first excited-state $S_1$ are interpreted to follow a torsionally driven lasing mechanism, with a Franck−Condon type "Stokes shift" of 5000 cm$^{-1}$ or more, measured as absorption−fluorescence peak displacement, with a corresponding displacement of the ASE laser spike from the absorption band F−C maximum.

**Acknowledgment.** We are greatly indebted to DGICYT of Spain for financial support (Project PB93-0280). J.C.V. acknowledges with thanks the granting of a Fulbright Scholarship by the Fulbright Commission and the Ministry of Education and Science of Spain. We are pleased to acknowledge the valuable assistance in laser optics by Drs. L. van de Burgt and David A. Gormin of the IMB Laser Laboratory. We thank Dr. R. M. Claramunt for a preliminary sample of 1-methyl-2-phenylimidazole which permitted us to make the comparisons given in Table 2.

## References and Notes

(1) Del Valle, J. C.; Kasha, M.; Catalán, J. *Chem. Phys. Lett.* **1996**, *263*, 154.
(2) Del Valle, J. C.; Kasha, M.; Catalán J. *J. Phys. Chem. A* **1997**, *101*, 3260.
(3) Khan, A. U.; Kasha, M. *Proc. Natl. Acad. Sci. U.S.A.* **1983**, *80*, 1767.
(4) Hoff, P. W.; Swingle, J. C.; Rhodes, C. K. *Appl. Phys. Lett.* **1973**, *23*, 245.
(5) Gordon, M.; Ware, W. R. *The Exciplex*. Academic Press: New York, 1975.
(6) Chou, P.; McMorrow, D.; Aartsma, T. J.; Kasha, M. *J. Phys. Chem.* **1984**, *88*, 4596.
(7) Rotkiewicz, K.; Grellmann, K. H.; Grabowski, Z. R. *Chem. Phys. Lett.* **1973**, *19*, 315.
(8) Heldt, J.; Gormin, J.; Kasha, M. *Chem. Phys.* **1989**, *136*, 321.
(9) Wiessner, A.; Huttmann, G.; Kuhnle, W.; Staerk, H. *J. Phys. Chem.* **1995**, *99*, 14923.
(10) Shank, C. V. *Rev. Mod. Phys.* **1975**, *47*, 649.
(11) Catalán, J.; Mena, E.; Fabero, F.; Amat-Guerri, F. *J. Chem. Phys.* **1992**, *96*, 2005.
(12) Siegman, A. E. *Lasers*; Kelly, A., Ed.; University Science Books: Mill Valley, CA, 1986.
(13) (a) Gaussian 94, Revision D.1; Frisch, M. J.; Trucks, G. W.; Schlegel, H. B.; Gill, P. M. W.; Johnson, B. G.; Robb, M. A.; Cheeseman, J. R.; Keith, T.; Petersson, G. A.; Montgomery, J. A.; Raghavachari, K.; Al-Laham, M. A.; Zakrzewski, V. G.; Ortiz, J. V.; Foresman, J. B.; Cioslowski, J.; Stefanov, B. B.; Nanayakkara, A.; Challacombe, M.; Replogle, E. S.; Gomperts, R.; Martin, R. L.; Fox, D. J.; Binkley, J. S.; Defrees, D. J.; Baker, J.; Stewart, J. P.; Head-Gordon, M.; Gonzalez, C.; Pople, J. A. Gaussian, Inc.: Pittsburgh PA, 1995. (b) Spartan version 4.1, Wavefunction Inc., Irvine, CA, 1995.
(14) Foresman, J. B.; Head-Gordon, M.; Pople, J. A.; Frisch, M. *J. Phys. Chem.* **1992**, *96*, 135.
(15) Schlegel, H. B. *J. Comput. Chem.* **1982**, *3*, 214.
(16) Pople, J. A.; Scott, A. P.; Wong, M. W.; Radom, L. *Isr. J. Chem.* **1993**, *33*, 345.
(17) All the harmonic vibrational frequencies, IR intensities, Raman scattering activities and spectral correlation will be included in a paper that is in preparation.
(18) Hallows, W. A.; Carpenter, G. B.; Pevear, K. A.; Sweigart, D. A. *J. Heterocycl. Chem.* **1994**, *31*, 899.
(19) Mulliken, R. S.; Roothaan, C. C. *J. Chem. Rev.* **1947**, *41*, 219.
(20) Gormin, D.; Sytnik, A. I.; Kasha, M. *J. Phys. Chem.* **1996**, *101*, 672.
(21) Godfrey, M.; Murrell, J. N. *Proc. R. Soc. London A* **1969**, *278*, 57, 71.
(22) Heldt, J.; Gormin, D.; Kasha, M. *Chem. Phys.* **1989**, *136*, 321. Cf. Figure 14 therein.